DESIGN OF A SUPERCONDUCTING FIELD MAGNET FOR A SYNCHRONOUS GENERATOR

Author: David L. Greene
Supervisor: Joseph L. Smith, Jr.
Associate Professor of
Mechanical Engineering
Submitted: 17 May 1968

DESIGN OF A SUPERCONDUCTING FIELD MAGNET FOR A SYNCHRONOUS GENERATOR

by

DAVID LOCKWOOD GREENE
LIEUTENANT, UNITED STATES NAVY
B.S., United States Naval Academy
(1963)

Submitted in Partial Fulfillment of the
Requirements for the Degree of
Naval Engineer and the Degree of
Master of Science in
Mechanical Engineering
at the
MASSACHUSETTS INSTITUTE OF TECHNOLOGY
May, 1968

Signature of Author: ______________________________
Department of Naval Architecture and Marine Engineering. May 18, 1968

Certified by: ______________________________
Thesis Supervisor

Certified by: ______________________________
Departmental Reader

Accepted by: ______________________________
Chairman, Departmental Committee on Graduate Students

DESIGN OF A SUPERCONDUCTING FIELD MAGNET FOR A SYNCHRONOUS GENERATOR

by

DAVID LOCKWOOD GREENE

Submitted to the Department of Naval Architecture and Marine Engineering on May 17, 1968 in partial fulfillment of the requirements for the Master of Science degree in Mechanical Engineering and the Professional Degree, Naval Engineer.

ABSTRACT

A superconducting field magnet is designed and constructed for use in a small synchronous generator of approximately 10 horsepower. The equations describing the field flux distribution are developed and compared with experimental results. The magnet is tested to insure superconducting operation in the generator system is possible. The performance of the magnet in the production of a superconducting field was found to be as predicted. For the construction of such fields in the future, an optimization scheme is presented for the selection of field geometry, as well as means for predicting stresses in the support structure.

Thesis Supervisor: Joseph L. Smith, Jr.
Title: Associate Professor of Mechanical Engineering

ACKNOWLEDGMENTS

The kind assistance of my thesis supervisor, Prof. Joseph L. Smith, Jr., Mr. Philip Thullen, and the staff of the Cryogenic Engineering Laboratory at the Massachusetts Institute of Technology in the preparation of this thesis is gratefully acknowledged.

LIST OF SYMBOLS

B	Flux density, Gauss
H	Field intensity, ampere-turns/meter
I_f	Field current, amperes
J_a	Armature current density, amperes/cm^2
J_f	Field current density, amperes/cm^2
L	Overall magnet length, inches
N_f	Number of turns in field winding
R_1	Inside field radius, inches
R_2	Outside field radius, inches
R_i	Inside armature radius, inches
R_o	Outside armature radius, inches
δ	Pole face angle, °
λ	Packing factor, conductors/cm^2
ρ	Radial distance, inches
ϕ	Clockwise angular measurement from magnetic axis of field winding, °

TABLE OF CONTENTS

INTRODUCTION

Recent investigations into the use of superconductors in electrical machines have indicated that generators can be constructed which will have higher output at greater efficiency, lower weight per unit of power and lower synchronous reactance than present generators. Future requirements for high capacity turbogenerators will demand the projected capabilities of such machines, and their application in gas turbine/electric drive propulsion plants for marine use may successfully overcome the present excessive weight problem of such plants.

The most promising use of superconductors in a generator is in the field windings, where the current is direct. Elimination of resistive losses in the field should increase generator efficiency measureably by reducing the power for excitation. The use of superconductors in the armature is not so promising, due to a number of problems associated with the use of superconductors with alternating current.

Since present design philosophy is content to leave the armature at ambient temperature, the remaining system design consideration is whether the armature or the field should be the rotating member. For large generators, the answer lies in the amount of power which must be transferred to or from the rotating member. If the armature rotated, the amount

is large, and the required brush contact area is large. However, if the field rotates, as is the case in present large generators, the power and brush area are small. Thus, the most practical configuration is with the field rotating, preferrably inside the armature to ease armature heating problems.

In order to uncover impediments to the construction of large superconducting machines, a small superconducting generator project was undertaken at the Massachusetts Institute of Technology. The project includes the design and construction of both the rotating dewar to house the superconducting field at liquid helium temperatures and the field magnet, as well as the future design and construction of a shielded armature. Figure 1 is a schematic diagram of the proposed system. Presently, the dewar and field assembly are intended for use with the stator from a two-pole, three-phase induction motor, rated at 7 horsepower. This thesis is concerned with the design and construction of the required field magnet, subject to the objective of producing the maximum possible field intensity.

Much of the work done in this thesis was based on a project conducted by the Avco-Everett Research Laboratory (1), under which a small, stationary field alternator was constructed. The analysis used in that project was extended to the present investigation, which deals with the inherently more practical rotating field machine.

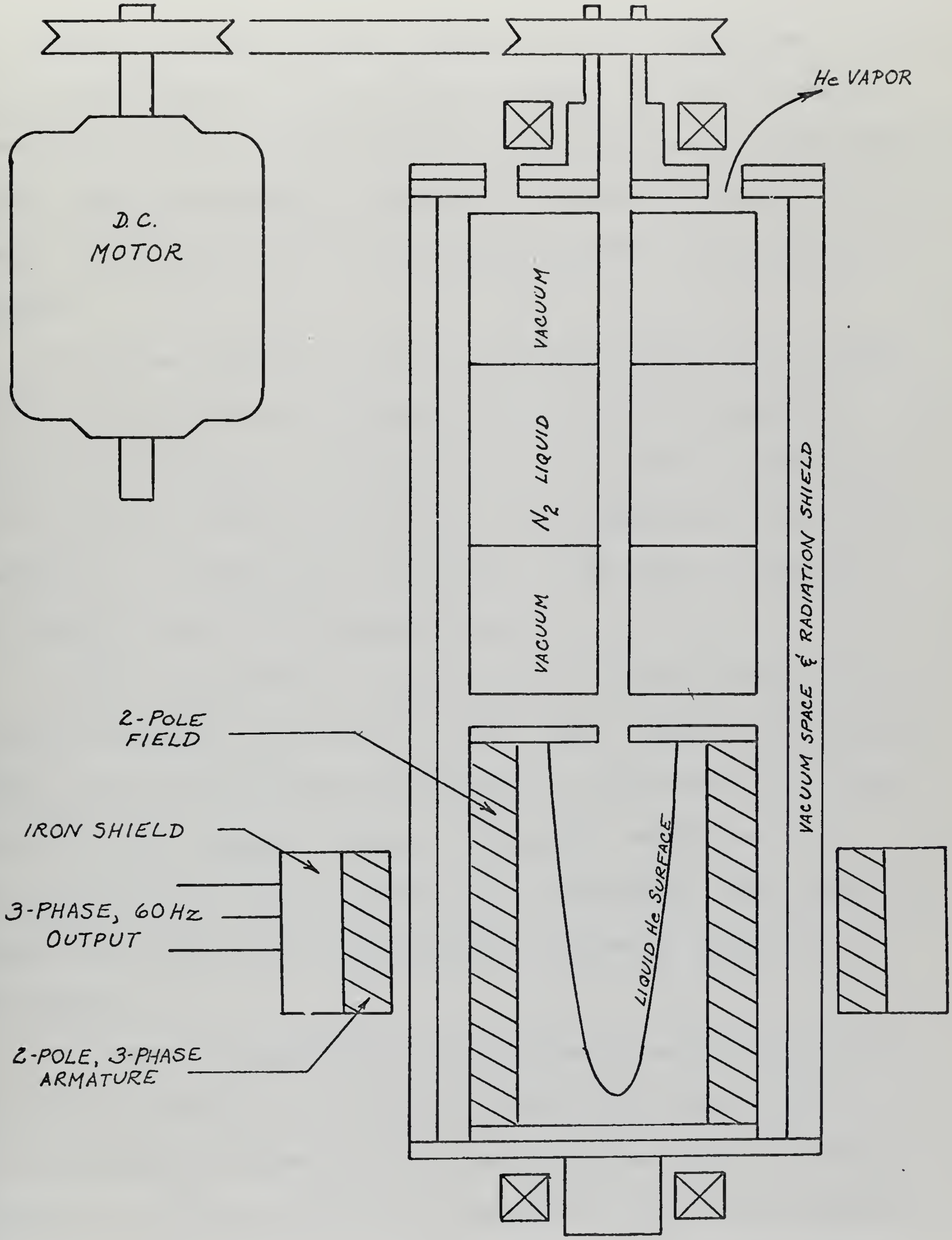

Figure 1. Proposed Superconducting Generator System

DESIGN SELECTION

Since the field magnet required by the design was to be incorporated with existing portions of the proposed generator system, certain design dimensions were immediately fixed. These included the length and outside diameter of the magnet. Additionally, the following demands were made of the design:

1. It was desired to keep the superconducting material within liquid helium throughout the period of operation. Since the configuration assumed by the surface of the liquid helium during rotation would be a steep parabola, all of the conductor, including the end turns, would have to reside in an annulus close to the dewar wall.

2. The dimensions of the stator to be used limited the outside diameter and length of the field. Because the liquid helium would not be replenished during the operation of the rotor for the initial trials, an annular thickness of 1" was selected to take advantage of a reasonably long operating time, and still allow a signigicant volume of conductor to be fitted.

3. Since the predicted field intensities for superconducting magnets are so large, the requirement for the use of ferromagnetic materials as flux paths has been eliminated. Therefore, unlike conventional machines, the forces generated by the field are carried by the conductors, rather than by any iron core, and the structure had to be configured to transfer the torque producing forces from the conductors to the shaft.

4. In order to keep the conductors at the required temperature for superconducting operation, adequate contact with the liquid helium must be maintained. This implied that passages would have to be provided in the structure to allow liquid helium to reach the conductor from the original introduction point on the central axis.

Consideration of several general design alternatives led to the configuration illustrated in Figure 2. The selection of the number of fins to be used and the dimensions required is covered in Appendix A. The two-pole field is produced by a superconducting wire winding on a cylindrical stainless steel tube with an outside diameter of 3". The wire is wound into segments created by fins extending radially outward from the tube. Each segment contains approximately 900 strands of .020" diameter wire. The wire is a .011" diameter core of niobium-40% titanium surrounded by copper and Formvar insulated.

As shown in Figure 2, the field is wound in six coils, each with approximately 900 turns. The winding was accomplished in place, in order to achieve the maximum space factor. The design assures that all of the conductor, including the end turns, is located in an annular volume 1" thick. Circular perforations in the central structural cylinder allow liquid helium to pass to the conductors for cooling. These passages cover approximately 20% of the cylinder surface.

The entire field is enclosed by a thin-walled stainless

steel tube to prevent radial movement of the conductors and to assure that helium vapor produced by boil-off will be confined to the region inside the liquid annulus.

The torque is transmitted by the radial fins from the conductor to the central cylinder and then to the dewar and shaft assembly by ¼" cap screws. The estimated torques and stresses experienced by the conductors and structure are computed in Appendix C.

The anticipated number of ampere-turns and the resulting field intensities which could be achieved by the design are presented in Appendix B.

The surface of all structural portions of the magnet is covered with a varnish type insulation to prevent shorting the winding to the structure. Additionally, the fins are wrapped with a Teflon and fiberglass tape to provide more insulating protection. Specifications for the wire used in the construction of the magnet are given in Appendix D.

Since the final measure of effectiveness of the magnet as a system component is the torque which it can produce, an optimization scheme is presented in Appendix E, proposing that there exists a particular geometry which will develop the maximum torque. The results of such a scheme will provide a check on the effectiveness of the thesis design.

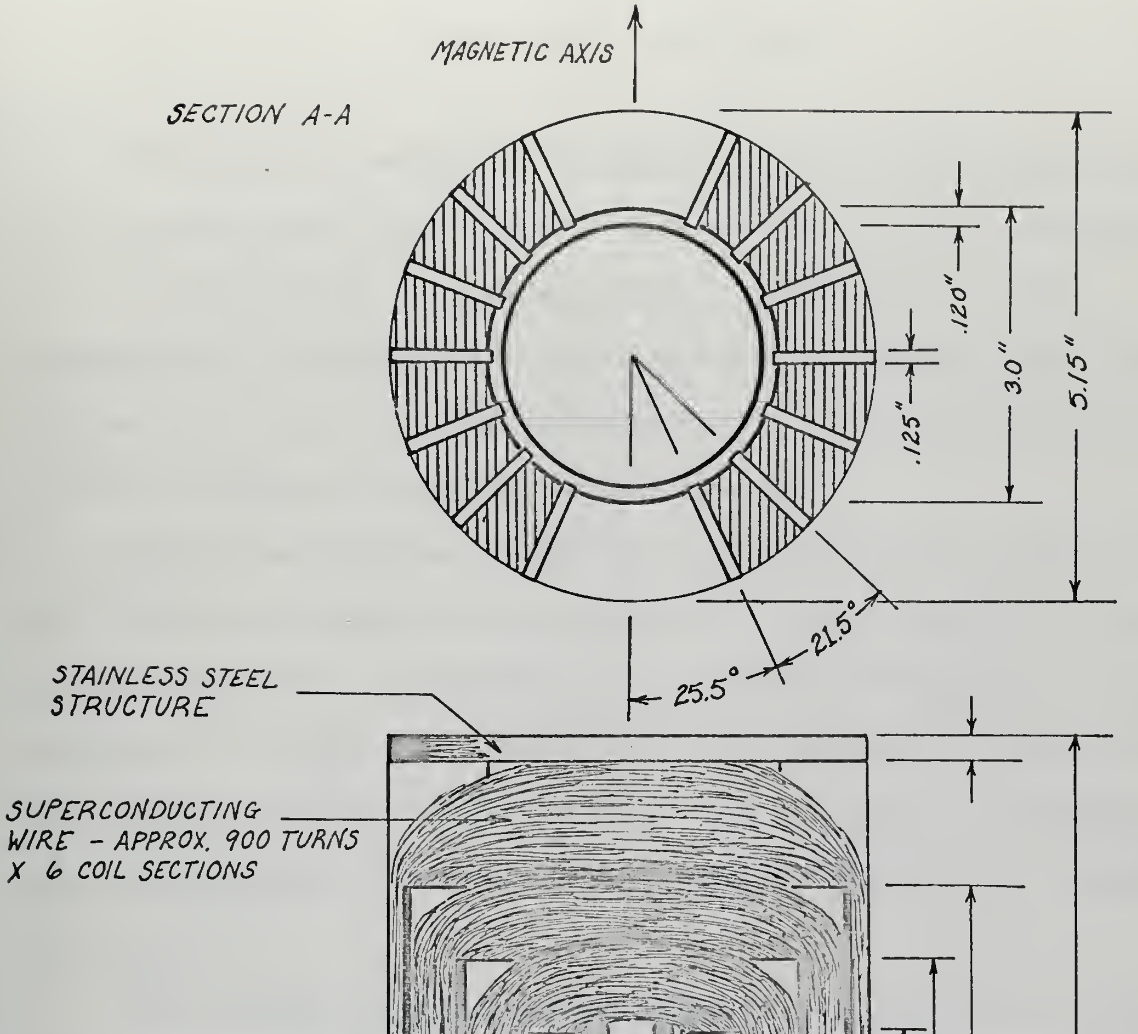

Figure 2. Two-pole, superconducting field magnet.

EXPERIMENTAL PROCEDURE

In order to evaluate the performance of the magnet, the flux pattern was measured and compared with that predicted by the theoretical values developed in Appendix B. The measurement was made at room temperature, because the field intensity is essentially independent of the environment, as long as magnetic material is not present.

Since the winding resistance was found to be 200 ohms, the flux was mapped at a low value of field current to prevent overheating the winding. To produce .20 amperes in the winding, 40 volts were required at the terminals. This voltage was obtained from a 110 volt d.c. source, and the excess power was dissipated in wire-wound and ceramic resistors, as shown in Figure 3.

The pattern was mapped by placing the probe of a rotating-coil flux meter in the field and reading the flux density directly. Readings were taken along three loci, as in Figure 4: radially from a pole face, circumferentially at the outside radius, and axially at the pole face and the outside radius.

To insure that the magnet would produce a superconducting field, a static test was made to determine the resistance of the winding in a bath of liquid helium. The winding was mounted in the dewar and energised with a small field current while submerged in liquid helium. The voltage and current at the field terminals were measured using the setup illustrated in Figure 5.

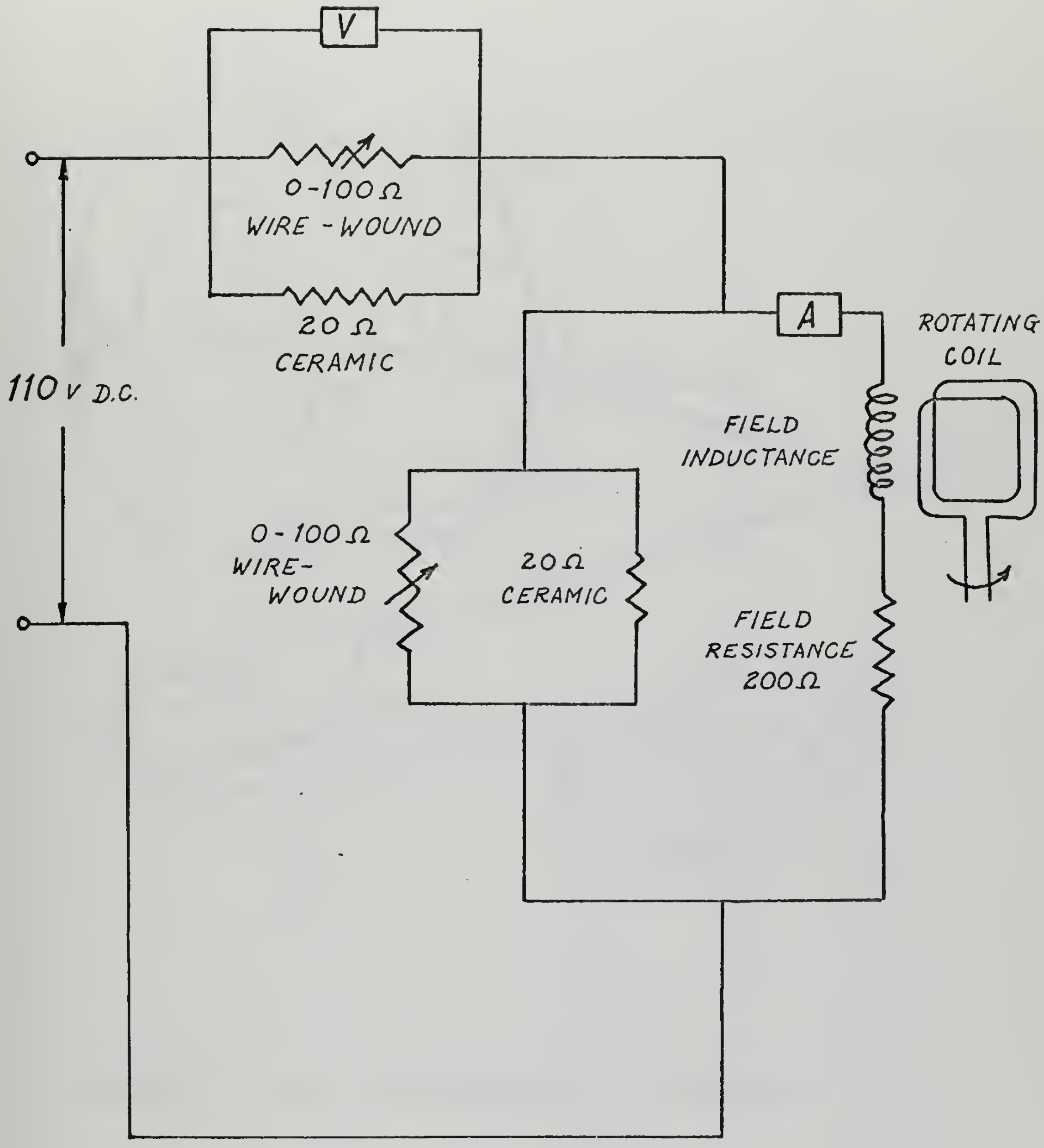

Figure 3. Circuit used to map flux pattern

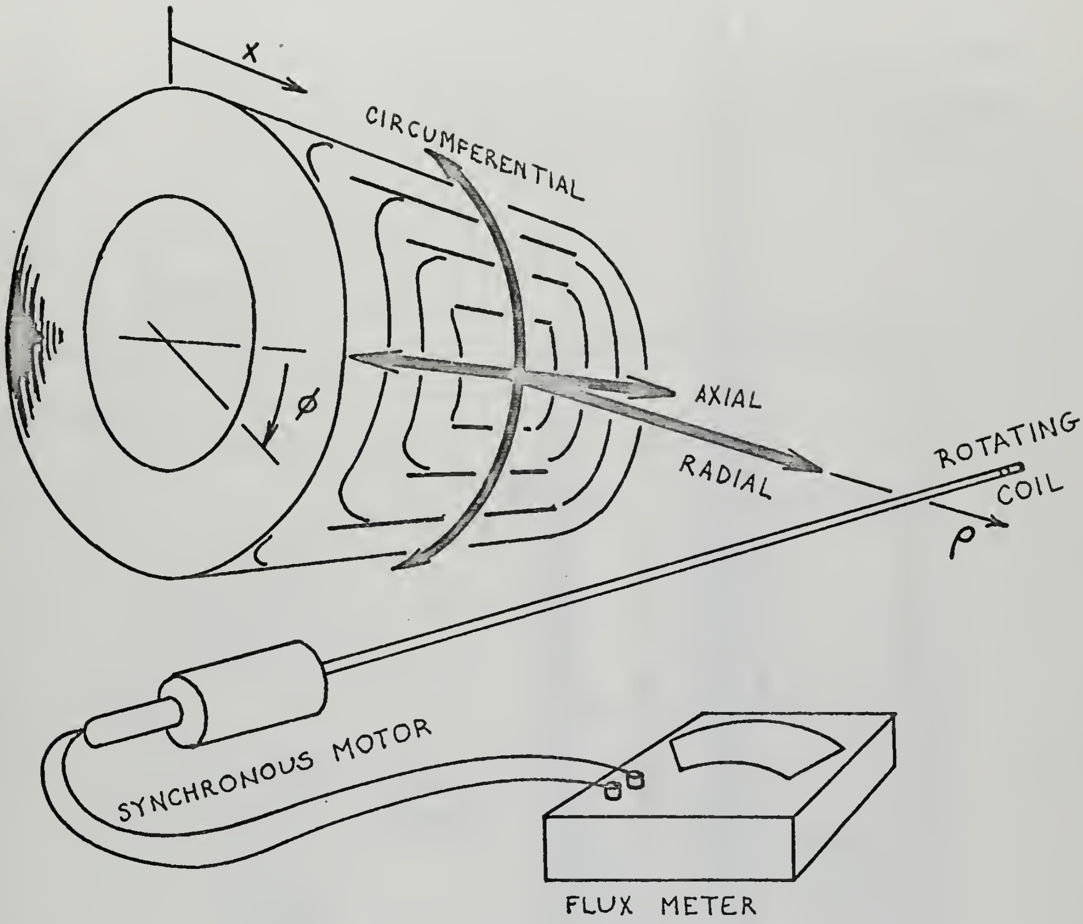

Figure 4. Loci for mapping flux pattern.

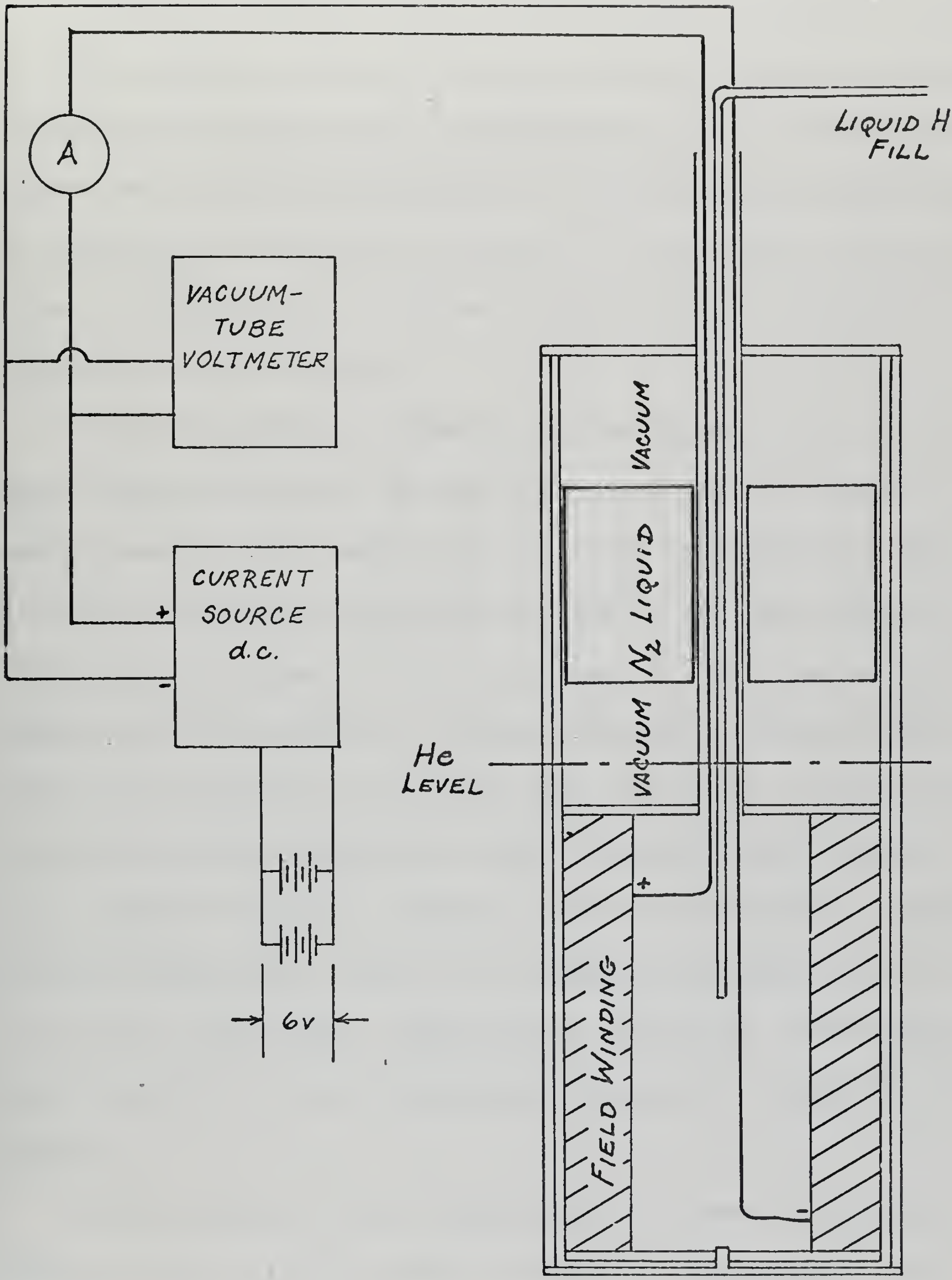

Figure 5. Apparatus for measurement of field resistance at liquid He temperature.

RESULTS

The flux density map is presented in Figures 6 through 8. The pattern along the radial axis is shown in Figure 6; the measured values are dots plotted with the predicted curve as derived in Appendix B. The circumferential pattern is similarly displayed in Figure 7. The axial flux distribution in Figure 8 is a curve faired through the experimental values of flux density.

The variation of electrical resistance with environment temperature for the winding is shown in Figure 9. Three measurements were taken: one at room temperature, the second at liquid nitrogen temperature, 80°K, and the last at a temperature assumed to be less than 9.7°K. The values of resistance obtained are plotted against a theoretical resistance curve which is divided into two parts. Above 9.7°K, the theoretical resistance curve assumes that copper is the sole current carrier, and the curve is based on a resistance versus temperature curve for copper from Scurlock (2). Below 9.7°K, the transition temperature of Nb-Ti, the curve assumes that the Nb-Ti core is superconducting and carrying all the current.

The results of the optimization scheme of Appendix E indicate that for the given number of conductors (5500) and the given outside radius (2.5"), a pole face angle of 10° and an inside radius of 1.875" would develop the maximum

torque when used with an armature whose current density is 10^2 amps/cm^2.

The results of the structural stress analysis in Appendix C show that the scantlings selected for construction are sufficient to carry the electromagnetic and rotational force loads. The maximum longitudinal bending stress anticipated in the support tube is 6200 psi at the mid-length. The maximum bending stress expected at the fin root is 1000 psi.

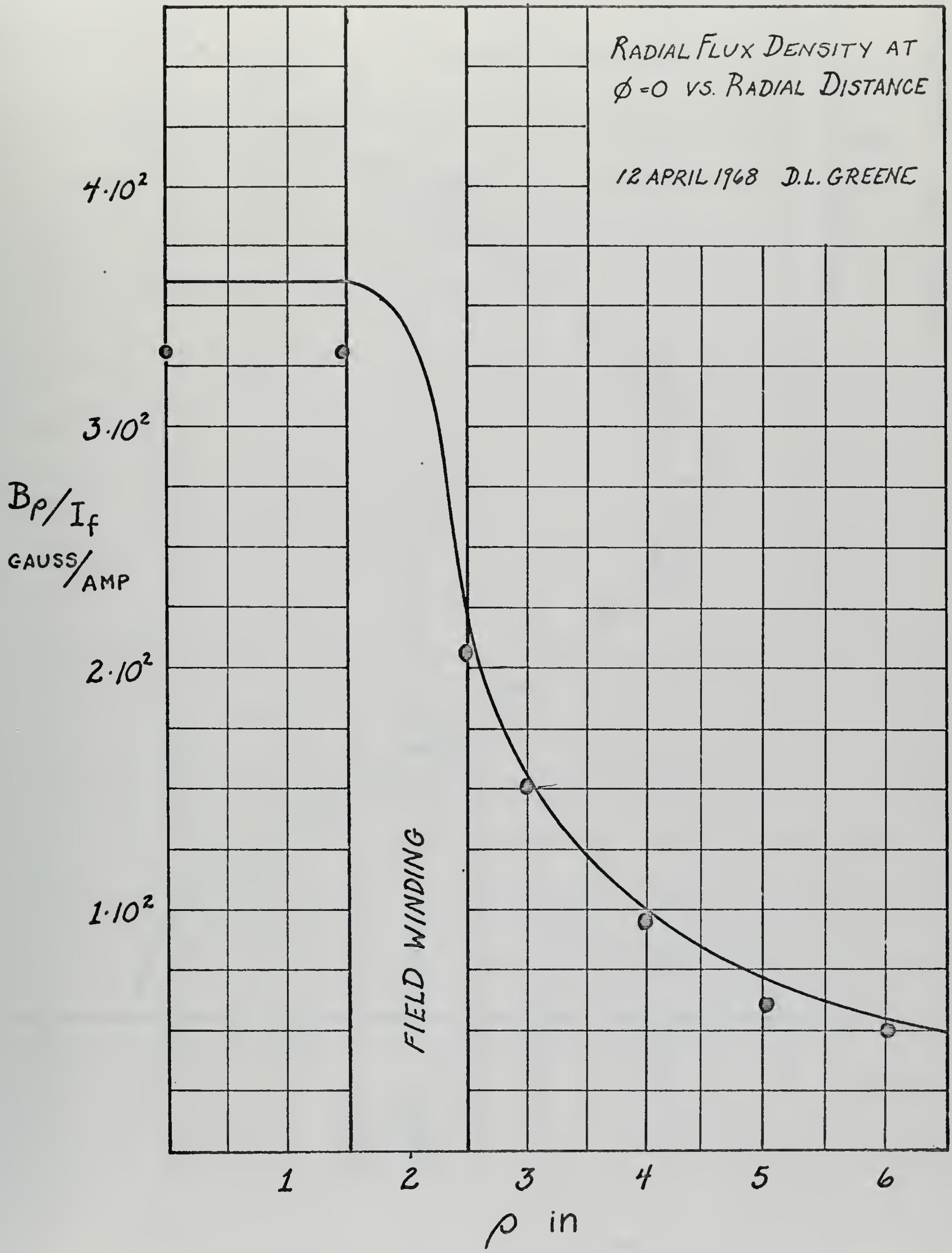

Figure 6. Plot of radial flux density as a function of of radial distance.

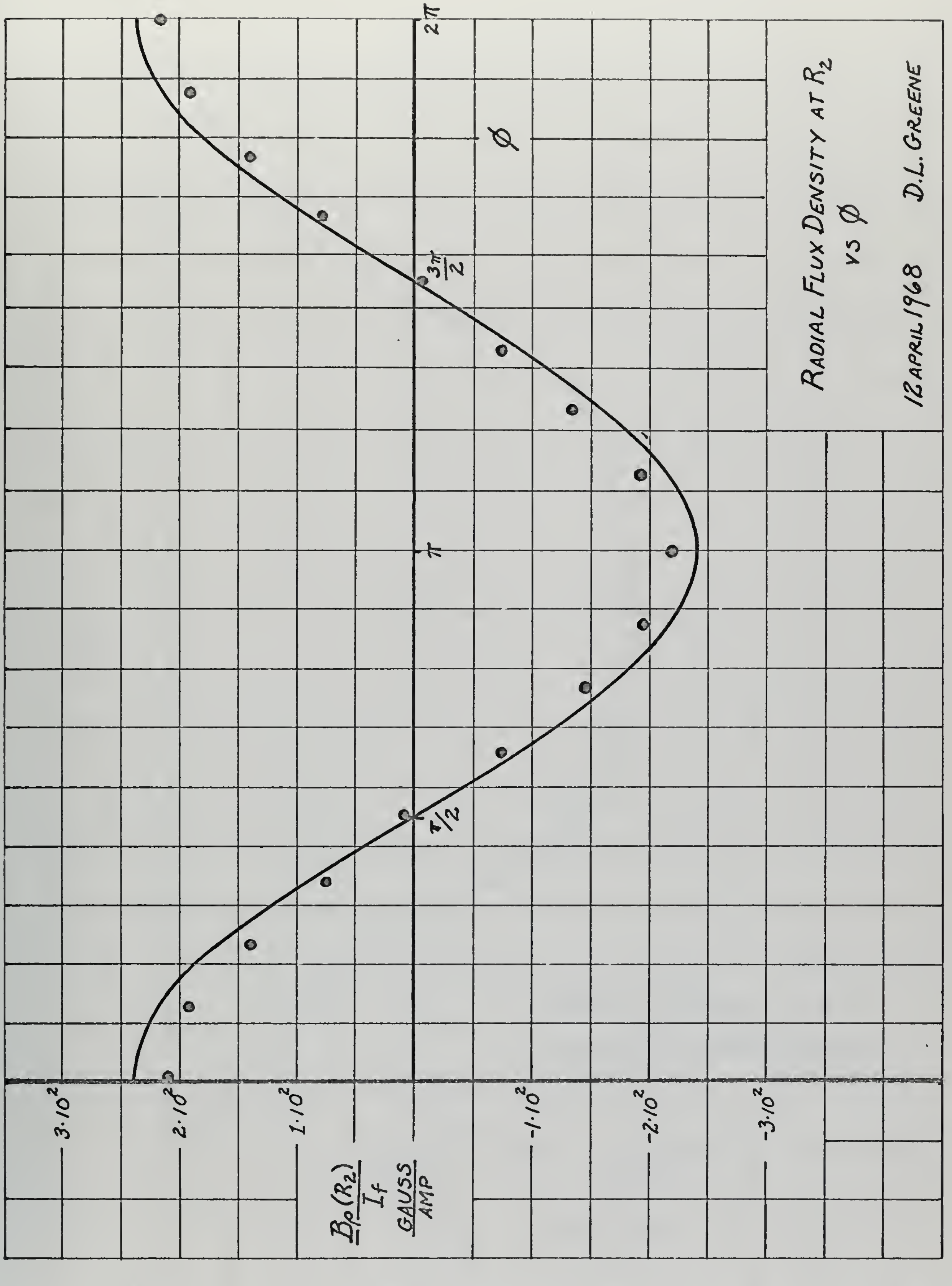

Figure 7. Plot of radial flux density around the circumference of field winding at radius R_2.

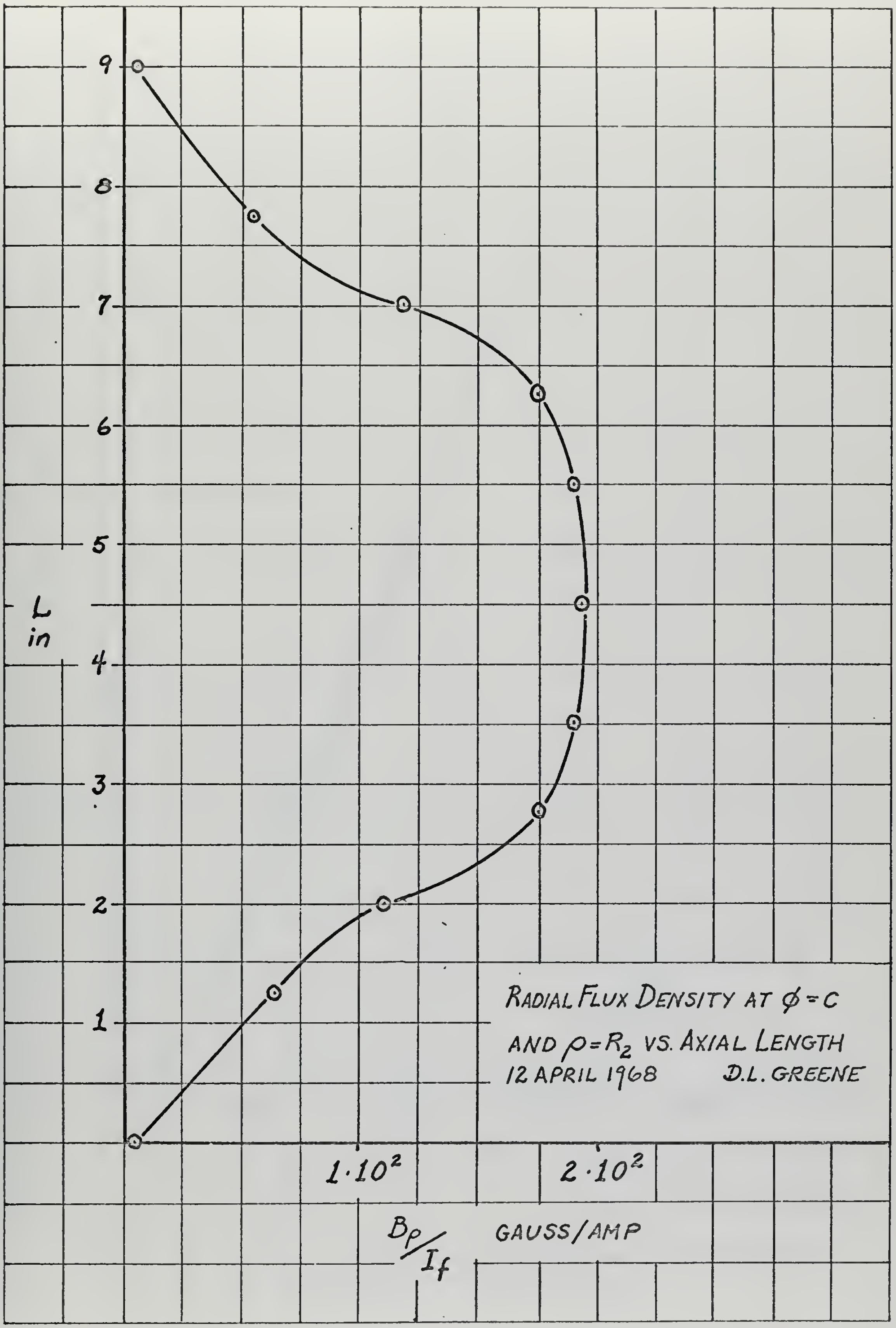

Figure 8. Plot of radial flux density along the longitudinal axis at radius R_2.

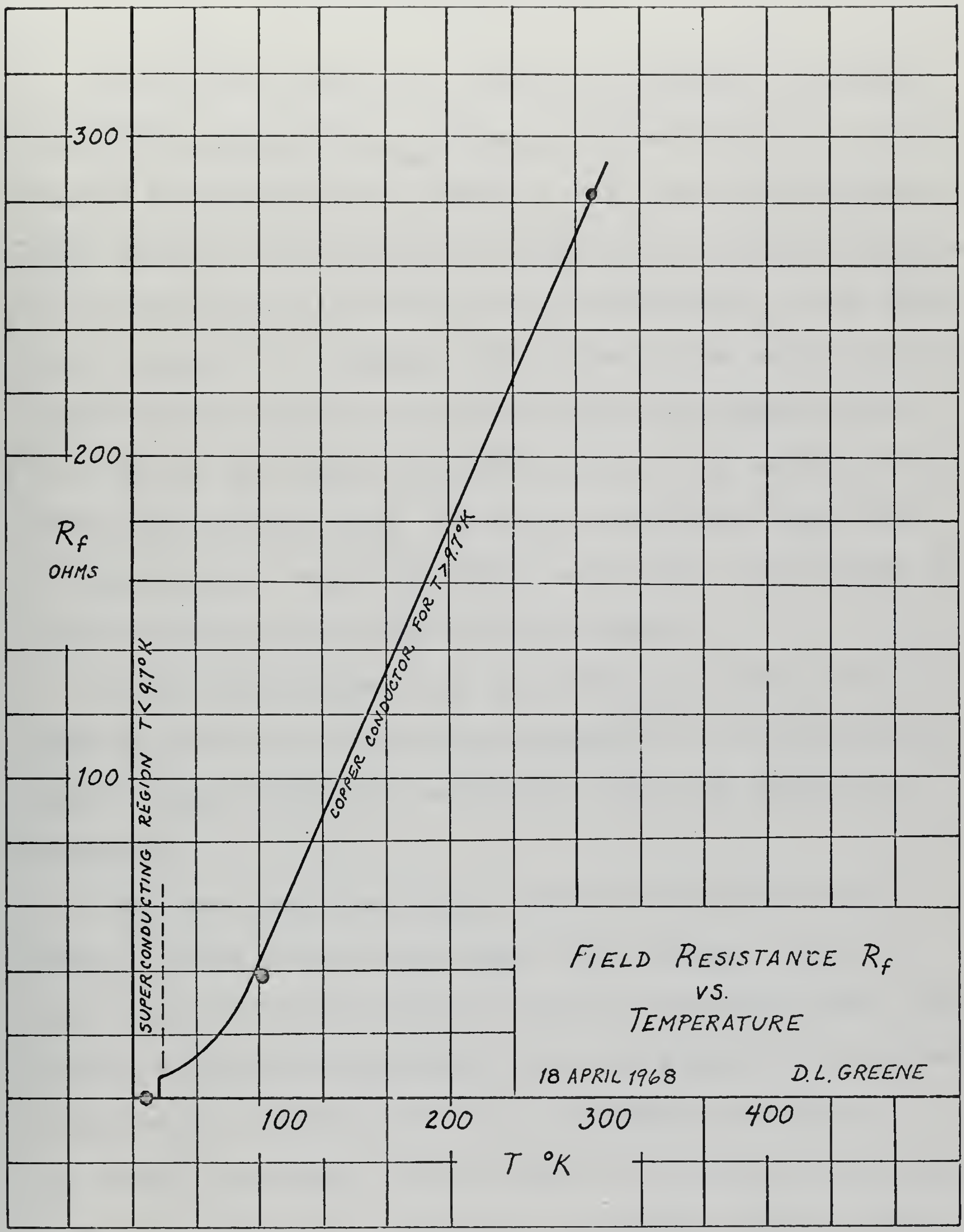

Figure 9. Plot of winding resistance as a function of environment temperature.

DISCUSSION OF RESULTS

As the flux maps show, there is essential agreement between the theoretical and measured distribution of flux density around the field winding. The axial distribution, which was not theoretically derived, is of interest because it allows some insight into the determination of the effective length of the winding. The shape of the curve indicates that the flux density is within 75% of the maximum value over 50% of the length and within 90% of the maximum over 40% of the length. Thus, the effective length might well be expressed as that length over which the flux density is within a given percentage of the maximum.

Since the resistance of the winding followed the expected pattern, it gave encouragement to the ability to achieve superconducting performance with the magnet as designed.

The fact that the torque would be optimized for a smaller value of pole face angle and a larger value of inside radius of the winding than were possible under the project constraints indicates that the design of a generator system should include the field optimization early in the design procedure. The existence of an optimum geometry should be sufficient motivation for careful field design, if the most efficient machine is to be realized.

CONCLUSIONS

The field winding developed under this project performed satisfactorily when examined for the production of flux intensity and for superconducting operation. The geometry of the field was not the optimum for the number of conductors used, since constraints of existing equipment prevented optimization. The design produced under this thesis is considered adequate to meet the requirements of producing the maximum field intensity for the generator system under development.

The maximum field intensity which can be produced is predicted to be 30 kG, using a field current of 80 amperes. For this field strength, the stresses experienced by the structure will probably produce deformations well below the elastic limit. The ease with which superconducting operation was achieved is interpreted as a prediction that such operation will be possible in rotation.

RECOMMENDATIONS

Several experiments should follow naturally from the work done in this thesis. The first would be to increase current to the nonrotating magnet during superconducting operation in order to find the maximum field strength and quenching current. Next the magnet should be rotated to insure that it is properly balanced, and any balance errors corrected. Then a stator might be fitted with a single turn coil to determine induced voltage when the field is rotated in the stator. Finally the field should be tested in a distributed, three-phase winding, in operational conditions of loading.

For larger machines in the future, it is felt that the windings should be made in hanks which can be fitted later into the slots, rather than being wound in place. Although there may be a slight reduction in the space factor which can be achieved, the savings in construction time and increased simplicity are more than offsetting.

When it becomes feasible to provide continuous replenishment of liquid helium, the inside radius of the winding can be reduced, providing greater volume for conductors and higher field intensity.

APPENDIX A

Selection of Design Dimensions

The dimension l_{pf} will determine l_{eff}, the effective length of the field, so it was felt that l_{pf} should be at least as long as the existing armature effective length, or approximately 3.5". L, the overall length, was reduced from 9" to 8" for the following calculations to account for the fact that the wire could not be wound to the ideal shape by hand. The relationship between the length required for end turns l_{et}, the overall length L and the pole face length l_{pf} becomes $l_{et} = \frac{1}{2}(L - l_{pf}) = 2.25"$.

The conductor wires from three slots must be able to pass through a cross section 1" x l_{et}", so the problem is simply to select a pole face angle δ (Figure A-2) which satisfies the equation

$$\frac{\pi}{4}(R_2^2 - R_1^2)\,\frac{90 - \delta}{90} = l_{et}$$

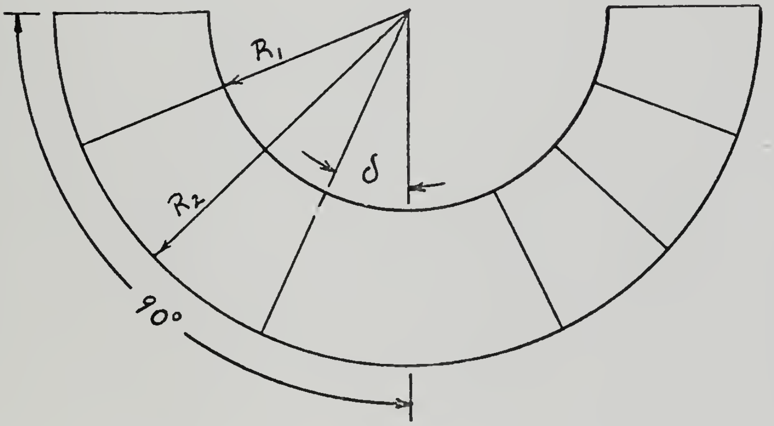

Figure A-2. Geometry for calculation of pole face angle.

APPENDIX B

Calculation of Flux Densities

Figure B-1 illustrates the nomenclature to be used in the development of expressions for the flux density distribution. It is first assumed that the field current distribution can be described by current sheets of thickness dr as shown in Figure B-1. These sheets have length l_{eff}, the effective length, and traverse the circumference from δ to $(180-\delta)$.

The current distribution can be expressed in a Fourier series determined as follows:

$$K(r) = \sum_{n\ odd} k_n \sin \frac{n\pi\phi}{L} \qquad L = \pi$$

$$k_n = \frac{2}{\pi}\int_0^{\pi} K(r) \sin n\phi d\phi$$

$$k_n = \frac{2}{\pi}\int_{\delta}^{180-\delta} J_f\, dr \sin n\phi d\phi$$

$$K(r) = \sum_{n\ odd} \frac{2\,J_f}{n\,\pi}\, dr \left[-\cos n(180-\delta) + \cos n\delta\right] \sin n\phi$$

Once the current distribution is known, the field intensity may be found by solving Laplace's Equation in spherical coordinates,

$$\frac{1}{\rho}\frac{\partial}{\partial\rho}\left(\rho\frac{\partial U}{\partial\rho}\right) + \frac{1}{\rho^2}\frac{\partial^2 U}{\partial\phi^2} = 0$$

where the field intensity $H = \nabla U$, such that

$$H_\rho = \frac{\partial U}{\partial\rho} \qquad \text{and} \qquad H_\phi = \frac{1}{\rho}\frac{\partial U}{\partial\phi}$$

The solution is subject to the following boundary conditions:

1. $\overline{H}$ is finite at $\rho = 0$
2. $H \rightarrow 0$ as $\rho \rightarrow \infty$

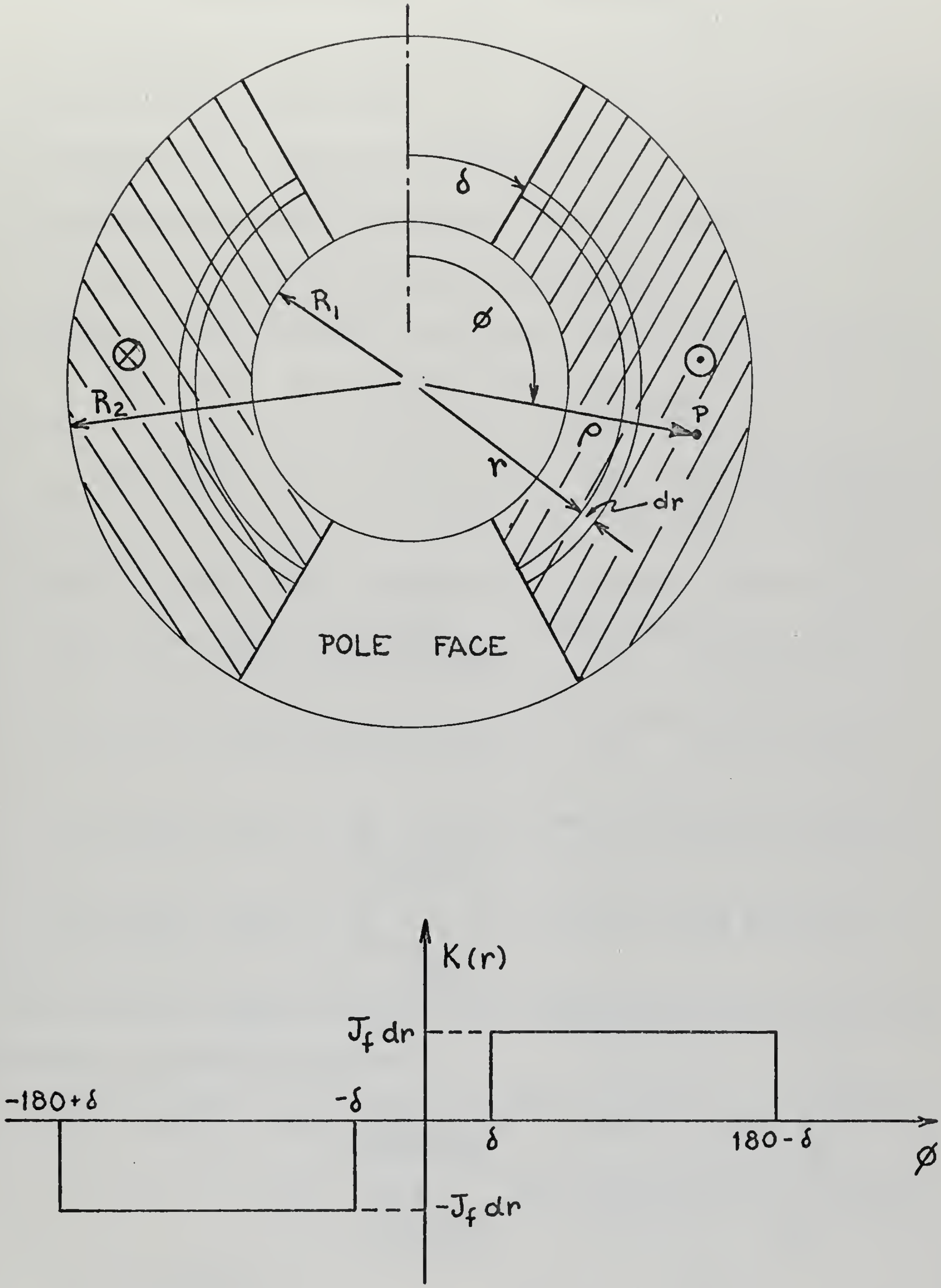

Figure B-1. Peripheral distribution of surface current density in sheet of thickness dr for two-pole field winding.

3. At the current sheet, H_ρ is continuous, i.e.,

$$H_\rho\,(\rho > r) - H_\rho\,(\rho < r) = 0$$

4. At the current sheet

$$H_\phi\,(\rho > r) - H_\phi\,(\rho < r) = K(r)$$

A product solution is assumed with the form:

$$U = (A\rho^{n} + B\rho^{-n})(C \sin n\phi + D \cos n\phi\,)$$

Applying the boundary conditions, the solution becomes:

$$\text{for } \rho < r, \quad U = \left(\frac{r^{-n+1}}{n}\rho^{n}\right)\left(-\sum_{n\ \mathrm{odd}} \frac{2\ J_f}{n\pi}\ dr \cos\delta\,\right)\cos n\phi$$

$$\text{for } \rho > r, \quad U = \left(\frac{r^{n+1}}{n}\rho^{-n}\right)\left(-\sum_{n\ \mathrm{odd}} \frac{2\ J_f}{n\pi}\ dr \cos\delta\,\right)\cos n\phi$$

Since $H = \nabla U$, the increment of intensity at P is

$$\text{for } \rho > r,\ dH_\rho = \sum_{n\ \mathrm{odd}} \frac{2J_f\ dr}{n\pi}\ r^{n+1}\ \rho^{-n-1}\cos\delta \cos n\phi$$

$$\text{for } \rho > r,\ dH_\phi = \sum_{n\ \mathrm{odd}} \frac{2J_f\ dr}{n\pi}\ r^{n+1}\ \rho^{-n-1}\cos\delta \sin n\phi$$

$$\text{for } \rho < r,\ dH_\rho = \sum_{n\ \mathrm{odd}} \frac{2J_f\ dr}{n\pi}\ r^{-n+1}\ \rho^{n-1}\cos\delta \cos n\phi$$

$$\text{for } \rho < r,\ dH_\phi = \sum_{n\ \mathrm{odd}} \frac{2J_f\ dr}{n\pi}\ r^{-n+1}\ \rho^{n-1}\cos\delta \sin n\phi$$

The field intensities are then found by integration over the current carrying annulus:

$$\text{for } \rho > R_2,\ H_\rho = \sum_{n\ \mathrm{odd}} \frac{2J_f}{n\pi}\rho^{-n-1}\ \cos\delta \cos n\phi \int_{R_1}^{R_2} r^{n+1}dr$$

$$H_\phi = \sum_{n\ \mathrm{odd}} \frac{2J_f}{n\pi}\rho^{-n-1}\ \cos\delta \sin n\phi \int_{R_1}^{R_2} r^{n+1}dr$$

for $R_1 < \rho < R_2$,

$$H = \sum_{n\ \mathrm{odd}} \frac{2J_f}{n\pi}\ \cos\delta \cos n\phi\left[\rho^{-n-1}\int_{R_1}^{R_2} r^{n+1}dr + \rho^{n-1}\int_{R_1}^{R_2} r^{-n+1}d\right.$$

$$H = \sum_{n\ \mathrm{odd}} \frac{2J_f}{n\pi}\ \cos\delta \sin n\phi\left[\rho^{-n-1}\int_{R_1}^{R_2} r^{n+1}dr + \rho^{n-1}\int_{R_1}^{R_2} r^{-n+1}d\right.$$

for $\rho < R_1$, $H_\rho = \sum\limits_{n \text{ odd}} \frac{2J_f \rho^{n-1}}{n^2 \pi} \cos\delta \cos n\phi \int_{R_1}^{R_2} r^{-n+1} dr$

$$H_\phi = \sum_{n \text{ odd}} \frac{2J_f \rho^{n-1}}{n^2 \pi} \cos\delta \sin n\phi \int_{R_1}^{R_2} r^{-n+1} dr$$

After integration, the equations become:

$\rho < R_1$: $H_\rho = \sum\limits_{n \text{ odd}} \frac{2J_f \rho^{n-1}}{n^2 \pi (2-n)} (R_2^{-n+2} - R_1^{-n+2}) \cos\delta \cos n\phi$

$$H_\phi = \sum_{n \text{ odd}} \frac{2J_f \rho^{n-1}}{n^2 \pi (2-n)} (R_2^{-n+2} - R_1^{-n+2}) \cos\delta \sin n\phi$$

$R_1 < \rho < R_2$:

$$H_\rho = \sum_{n \text{ odd}} \frac{2J_f \rho}{n^2 \pi (4-n^2)} \left[-2n + (2+n)\left(\frac{R_2}{\rho}\right)^{-n+2} - (2-n)\left(\frac{R_1}{\rho}\right)^{n+2}\right] \cos\delta \cos n\phi$$

$$H_\phi = \sum_{n \text{ odd}} \frac{2J_f \rho}{n^2 \pi (4-n^2)} \left[4 + (2+n)\left(\frac{R_2}{\rho}\right)^{-n+2} - (2-n)\left(\frac{R_1}{\rho}\right)^{n+2}\right] \cos\delta \sin n\phi$$

$R_2 < \rho$: $H_\rho = \sum\limits_{n \text{ odd}} \frac{2J_f \rho^{-n-1}}{n^2 \pi (n+2)} (R_2^{n+2} - R_1^{n+2}) \cos\delta \cos n\phi$

$$H_\phi = \sum_{n \text{ odd}} \frac{2J_f \rho^{-n-1}}{n^2 \pi (n+2)} (R_2^{n+2} - R_1^{n+2}) \cos\delta \sin n\phi$$

To evaluate these equations for the design selected, J_f must be computed. Since the total ampere-turns are equal to the current density integrated over the sectional area of the conductor volume, the ampere-turns are

$$N_f I_f = \frac{J_f \pi (R_2^2 - R_1^2)}{2} \frac{(90^\circ - \delta^\circ)}{90^\circ}.$$

For the design as constructed, $N_f = 5500$, $R_1 = 3.82$ cm, $R_2 = 6.35$ cm, $\delta = 25.5^\circ$. These values may be used to solve for J_f, which becomes $J_f = 1.98\ 10^2\ I_f$ amp/cm^2. It is most informative to obtain the ratio of flux density to field current for the field, so the relationship $B = \mu_0 H$ is employed. With this relationship, the value of J_f computed above, and the

field dimensions, the field intensity equations may be transformed to a description of the flux density distribution for the field magnet. Since the measured flux distribution is to be compared with these distributions, it is sufficient to consider only the fundamental component of the flux (i.e. $n = 1$). Thus, for $\rho < R_1$,

$$B_\rho = \frac{2J_f\mu_0}{\pi}(R_2 - R_1)\cos\delta\cos\phi$$

$$B_\phi = \frac{2J_f\mu_0}{\pi}(R_2 - R_1)\cos\delta\sin\phi$$

for $R_1 < \rho < R_2$,

$$B_\rho = \frac{2J_f\mu_0\rho}{3\pi}\left[-2 + \frac{3R_2}{\rho} - \left(\frac{R_1}{\rho}\right)^3\right]\cos\delta\cos\phi$$

$$B_\phi = \frac{2J_f\mu_0\rho}{3\pi}\left[4 - \frac{3R_2}{\rho} - \left(\frac{R_1}{\rho}\right)^3\right]\cos\delta\sin\phi$$

for $R_2 < \rho$,

$$B_\rho = \frac{2J_f\mu_0}{3\pi\rho^2}(R_2^3 - R_1^3)\cos\delta\cos\phi$$

$$B_\phi = \frac{2J_f\mu_0}{3\pi\rho^2}(R_2^3 - R_1^3)\cos\delta\sin\phi$$

If these equations are evaluated at the pole face ($\phi = 0$), an expression for the radial flux distribution is obtained:

for $\rho < R_1$ $\quad B_\rho = 3.60\ 10^2\ I_f$ Gauss

for $R_1 < \rho < R_2$ $\quad B_\rho = 48.2\ I_f\left[-2\rho + 19.1 - \frac{55.5}{\rho^2}\right]$ Gauss

for $R_2 < \rho$ $\quad B_\rho = \frac{9.60\ 10^3}{\rho^2}\ I_f$ Gauss

where ρ is in centimeters. The circumferential distribution at any radius can be obtained by using the above values as maxima and applying the relationship $B_\rho(\phi) = B_{\rho\,max}\cos\phi$. The values so obtained will be a reasonable approximation over the effective length in the axial direction.

APPENDIX C

Calculation of Principal Stresses in the Field Assembly

The stresses in the field assembly can be convieniently separated into two catagories, those arising from the electromagnetic forces and those due to the rotation, and then superimposed to yield the total stress. Of greatest interest are the stresses in the central support tube and in the cantilevered fins. The first examination, then, is the determination of the stresses in the central support tube due to the electromagnetic forces. These forces originate in the conductors and are transmitted to the structure, much like a pressure distribution over the surface.

The force on a differential volume in the radial direction is

$$d\bar{F}_\rho = \bar{J} \times \bar{B}_\phi dV$$

With the expression for the fundamental component of tangential flux density derived from Appendix B and (1), the differential force becomes

$$dF_\rho = \left\{ \frac{2\mu J_f^2}{3\pi} \left[-2 + \frac{3R_2}{\rho} - \left(\frac{R_1}{\rho}\right)^3 \right] \rho \sin\phi \cos\delta - \frac{3\mu}{2\pi} J_f J_a (R_o - R_i)(R_2^3 - R_1^3) \cos\phi \right\} dV$$

The force distribution per unit length as a function of ϕ may be found by integrating the above differential over the thickness of the conductor volume. The result of this integration is

$$F_\rho(\phi) = \frac{2\mu_o}{3\pi} J_f^2 \left[-\frac{2}{3}(R_2^3 - R_1^3) + \frac{3}{2} R_2 (R_2^2 - R_1^2) - R_1^3 \ln(R_2 - R_1) \right] \cos\delta \sin\phi$$

$$- \frac{3\mu_o}{4\pi} J_f J_a (R_o - R_1)(R_2 - R_1) \cos\phi \; .$$

If a value of 10^2 amp/cm^2 is assumed for armature current density and $1.98\ 10^2\ I_f$ amp/cm^2 for field current density as found in Appendix B, then for the geometry of the generator system anticipated by the MIT project, where $R_o - R_i = 2.54$ cm, the force distribution on the outer surface of the central support tube is given by

$$F_\rho = .0617\ I_f^2 \sin\phi - .0396\ I_f \cos\phi$$

From Appendix B, the maximum field density is given by $B_\rho = 3.60\ 10^2\ I_f$. If this relationship is plotted on the short sample performance characteristic of Figure D-1, the intersection gives the maximum allowable field current, approximately 80 amperes. With this value of I_f, the force can be closely approximated by the first term only,

$$F_\rho(\phi) = 394 \sin\phi \qquad \text{for } 0 < \phi < \pi$$

$$-394 \sin\phi \qquad \text{for } \pi < \phi < 2\pi \text{, in newtons/radian.}$$

From Wang (3), the equilibrium equations for circular cylindrical shells are

$$\frac{\partial^2 u}{\partial x^2} + \frac{1-\nu}{2a^2}\frac{\partial^2 u}{\partial \phi^2} + \frac{1+\nu}{2a}\frac{\partial^2 v}{\partial x \partial \phi} - \frac{\nu}{a}\frac{\partial w}{\partial x} + p_1\frac{(1-\nu^2)}{Eh} = 0$$

$$\frac{1+\nu}{2a}\frac{\partial^2 u}{\partial x \partial \phi} + \frac{1-\nu}{2}\frac{\partial^2 v}{\partial x^2} + \frac{1}{a^2}\frac{\partial^2 v}{\partial \phi^2} - \frac{1}{a^2}\frac{\partial w}{\partial \phi} + \frac{h^2}{12a^2}\left(\frac{\partial^3 w}{\partial x^2 \partial \phi} + \frac{\partial^3 w}{a^2 \partial \phi^3}\right)$$
$$+ \frac{h^2}{12a^2}\left(\frac{1-\nu}{2}\frac{\partial^2 v}{\partial x^2} + \frac{1}{a^2}\frac{\partial^2 v}{\partial \phi^2}\right) + p_2\frac{(1-\nu^2)}{Eh} = 0$$

$$\nu\frac{\partial u}{\partial x} + \frac{\partial v}{a \partial \phi} - \frac{w}{a} - \frac{h^2}{12a^2}\left(a^3\frac{\partial^4 w}{\partial x^4} + 2a\frac{\partial^4 w}{\partial x^2 \partial \phi^2} + \frac{\partial^4 w}{a\,\partial \phi^4}\right)$$
$$- \frac{h^2}{12}\left(\frac{1}{a}\frac{\partial^3 v}{\partial x^2 \partial \phi} + \frac{1}{a^3}\frac{\partial^3 v}{\partial \phi^3}\right) + ap_3\frac{(1-\nu^2)}{Eh} = 0,$$

where u, v, and w are deflections in the x (axial), ϕ (tangential), and ρ (radial) directions, respectively. If the ends of the cylinder are assumed to be simply supported, then the boundary conditions at the ends may be expressed by v = 0, w = 0, and the shear force and bending moments are zero at x = 0 and x = L. Thus a solution of the form of three Fourier series may be used to describe the deflections:

$$u = \sum_{m=1}^{\infty} \sum_{n=0}^{\infty} A_{mn} \cos n\phi \cos \frac{m\pi x}{L}$$

$$v = \sum_{m=1}^{\infty} \sum_{n=0}^{\infty} B_{mn} \sin n\phi \sin \frac{m\pi x}{L}$$

$$w = \sum_{m=1}^{\infty} \sum_{n=0}^{\infty} C_{mn} \cos n\phi \sin \frac{m\pi x}{L}$$

The loading may also be described by a Fourier series obtained in the usual way:

$$p_1 = 0, \; p_2 = 0, \; p_3 = \begin{array}{ll} 394 \sin\phi & \text{for } 0 < \phi < \pi \\ -394 \sin\phi & \text{for } \pi < \phi < 2\pi \end{array}$$

$$p_3 = \sum_{m=1}^{\infty} \sum_{n=0}^{\infty} D_{mn} \cos n\phi \sin \frac{m\pi x}{L}$$

with $$D_{mn} = \frac{8}{m\pi^2} \int_0^{\pi} 394 \sin\phi \cos n\phi \, d\phi$$

Evaluation of the integral leads to the series

$$p_3 = \sum_m \sum_n \frac{3152}{m\pi^2} \frac{\cos n\phi + 1}{(1-n)(1+n)} \cos n\phi \sin \frac{m\pi x}{L}$$

Substitution of the series expressions for u, v, w, and p_3 into the equilibrium equations gives three homogeneous

equations in A_{mn}, B_{mn}, and C_{mn}. Values for u, v, and w may be obtained with sufficient accuracy by evaluation of the coefficients at m = 1,2 and n = 0,1,2; since the series converge rapidly. The primary stress in the central structural tube will be due to the longitudinal bending moment, which is given by Wang (3) as

$$(M_x)_{max} = \frac{Eh^3}{12(1-\nu^2)}\left[\frac{\partial^2 w}{\partial x^2} + \frac{\nu}{a^2}\left(\frac{\partial v}{\partial \phi} + \frac{\partial^2 w}{\partial \phi^2}\right)\right]$$

This expression may be evaluated for the particular application of this design, using the deflection series values and other parameters as follows:

E (modulus of elasticity)	= 30×10^6 psi
h (tube wall thickness)	= .120 inches
ν (Poisson's ratio)	= .25
a (tube radius)	= 1.5 inches
L (tube length)	= 9 inches ,

resulting in a bending moment of 15 inch-pounds. Wang shows that the stress associated with the maximum longitudinal bending moment is

$$\sigma_x = \frac{6}{h^2} M_{x_{max}} \quad \text{psi}$$

Thus, σ_x = 6200 psi at mid length.

The longitudinal stress due to the rotation of a tubular shaft may now be added to that due to the electromagnetic stresses. The stress may be calculated using the formula

$$\sigma_x = (3-2\nu)\frac{\nu\rho w^2}{4(1-\nu)}\left(b^2 + a^2 - \frac{2r^2}{3-2\nu}\right),$$

which assumes that the ends of the tube are constrained longitudinally. For the present design $\rho = .278\ \mathrm{lb/in}^3$, $\omega = 3600$ RPM, b (the inside tube radius) = 1.38 in, and the stress is determined for r = b. This stress is found to be small, less than 100 psi, in comparison to almost 10,000 psi due to the electromagnetic forces. The rotational stress is therefore neglected, and the working stress of the cylinder is estimated to be an order of magnitude lower than the yield stress of the stainless steel used in the support construction.

To estimate the bending stress in the radial fins, there are two sources of loading which must be considered. The first results from the forces which produce the machine torque and the second are the field self-forces. In analyzing the first, it is assumed that the machine torque is produced by a uniformly distributed load on the fins (or an equivalent point load at the mid-span of each fin). From Appendix E, the torque is found to be

$$T = \frac{2\mu}{\pi} J_f J_a \,(R_o - R_i)(R_2^3 - R_1^3)\cos\delta \; l_{eff}$$

For the following values:

$J_f = 1.98\ 10^2\ I_f\ \mathrm{amps/cm}^2$

$J_a = 10^2\ \mathrm{amps/cm}^2$

l_{eff} (effective length) = 4 in = .1 meter

$I_f = 80$ amps,

the torque becomes T = 40 ft-lb.

Since this torque will be carried by 12 of the 14 fins,

3.3 ft-lb is the torque on each fin. The radial center of each fin is at a 2 inch radius, so that the equivalent load is a concentrated force of 20 pounds at the mid-radius of the conductor annulus. The bending moment resulting from this force is .84 ft-lb. The worst stress condition will occur at the intersection of the shortest fin and the support tube, since the shortest fin will have the smallest moment of inertia. Figure C-1 shows the geometry of the point being examined. With $\sigma = \frac{My}{I}$ and $I = \frac{bh^3}{12}$, the stress is found to be 100 psi, well within the tolerances expected of the weld and fin material.

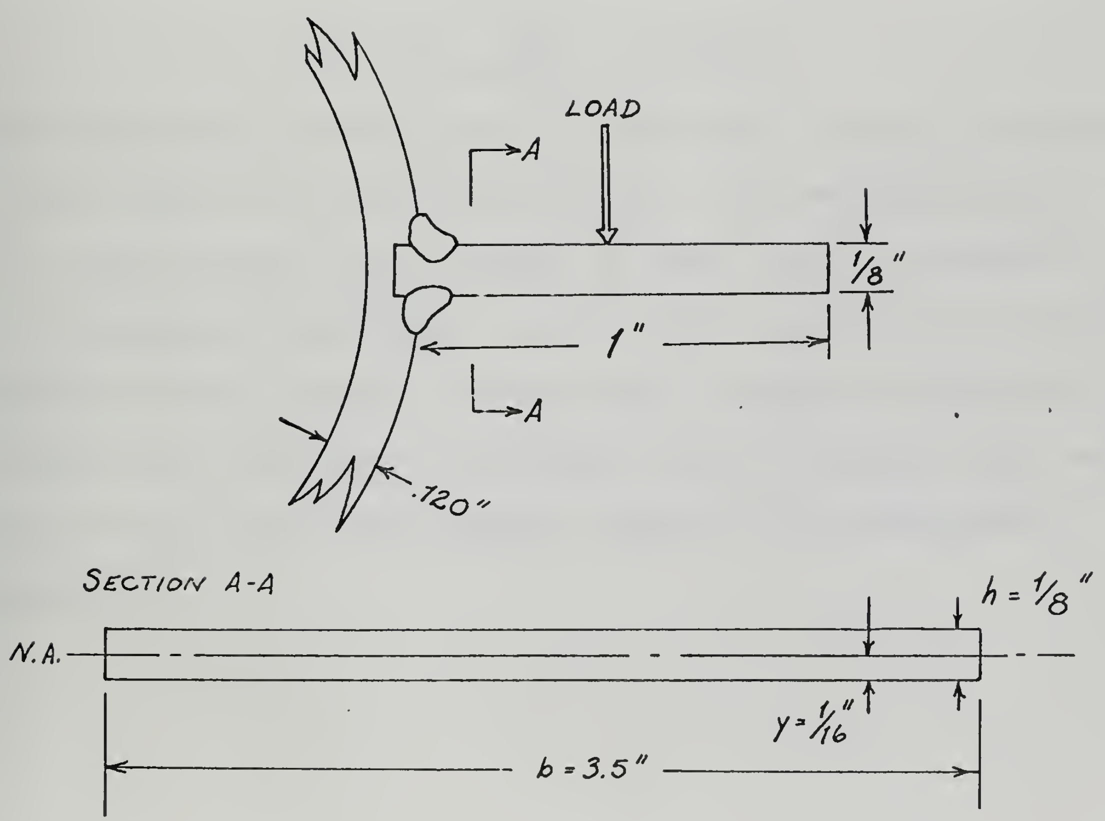

Figure C-1. Geometry at Fin Root

In examining the fin loading due to the field self-forces, the differential of force on the conductors can be written

$$d\bar{F}_\phi = \bar{J}_f \times \bar{B} \; dV$$

The force on the conductors in the segment from ϕ_1 to ϕ_2 can be found by evaluation of the integral

$$F_\phi = \int_0^L \int_{\phi_1}^{\phi_2} \int_{R_1}^{R_2} \bar{J}_f \times \bar{B}_\rho \, \rho \, d\rho \, d\phi \, dl \; ,$$

which becomes

$$F_\phi = \int_0^L \int_{\phi_1}^{\phi_2} \int_{R_1}^{R_2} \frac{2\mu_0}{3\pi} J_f^2 \left[-2 + \frac{3R_2}{\rho} - \left(\frac{R_1}{\rho}\right)^3 \right] \rho^2 \cos\delta \, \cos\phi \;\; d\rho \, d\phi \, dl$$

when the expression for B is inserted. With the proper values of field variables applied, the expression becomes

$$F = .951 \; I_f^2 \; \sin\phi \Big]_{\phi_1}^{\phi_2} \quad \text{newtons.}$$

This expression is maximized for the fins closest to the pole face, where $\phi_1 = 25.5^\circ$ and $\phi_2 = 47^\circ$. The maximum value is $F = 625$ newtons or 275 pounds. If this force is assumed to be uniformly distributed over the fin, the resulting bending stress at the fin root is 1000 psi, an order of magnitude larger than the stress resulting from the torque load, but still well within the expected limits of the structural material.

APPENDIX D

Superconductor Specifications

The following data are taken from an advance technical bulletin describing Nb-Ti Supergenic Wire, Type SG-100D, produced by Avco-Everett Research Laboratory.

a. Material - Supergenic Wire is a composite superconducting wire composed of copper clad Nb-40% Ti. This material permits the economical manufacture of superconducting coils up to 100 kG.

b. Dimensions and Weight - Type SG-100D has a 0.020" outside diameter and contains a 0.011" core of Nb-40% Ti. The insulation is a one mil coating of Formvar.

c. Design Stress - A design stress between 10,000 psi and 15,000 psi is currently recommended on the total cross section.

d. Stability - Type SG-100D is fully stable in short-sample tests and can be incorporated into fully stable coils when adequate cooling is provided.

e. Handling - Supergenic Wire is a rugged, ductile material. Both copper and niobium titanium are ductile materials and may be handled with conventional winding machines. Lapped soldered joints are permitted and may be wound into a properly designed coil.

f. Performance - Developmental type SG-100D short-sample performance is shown in Figure D-1. A manufacturing tolerance of ±10% currently is typical of developmental quantities.

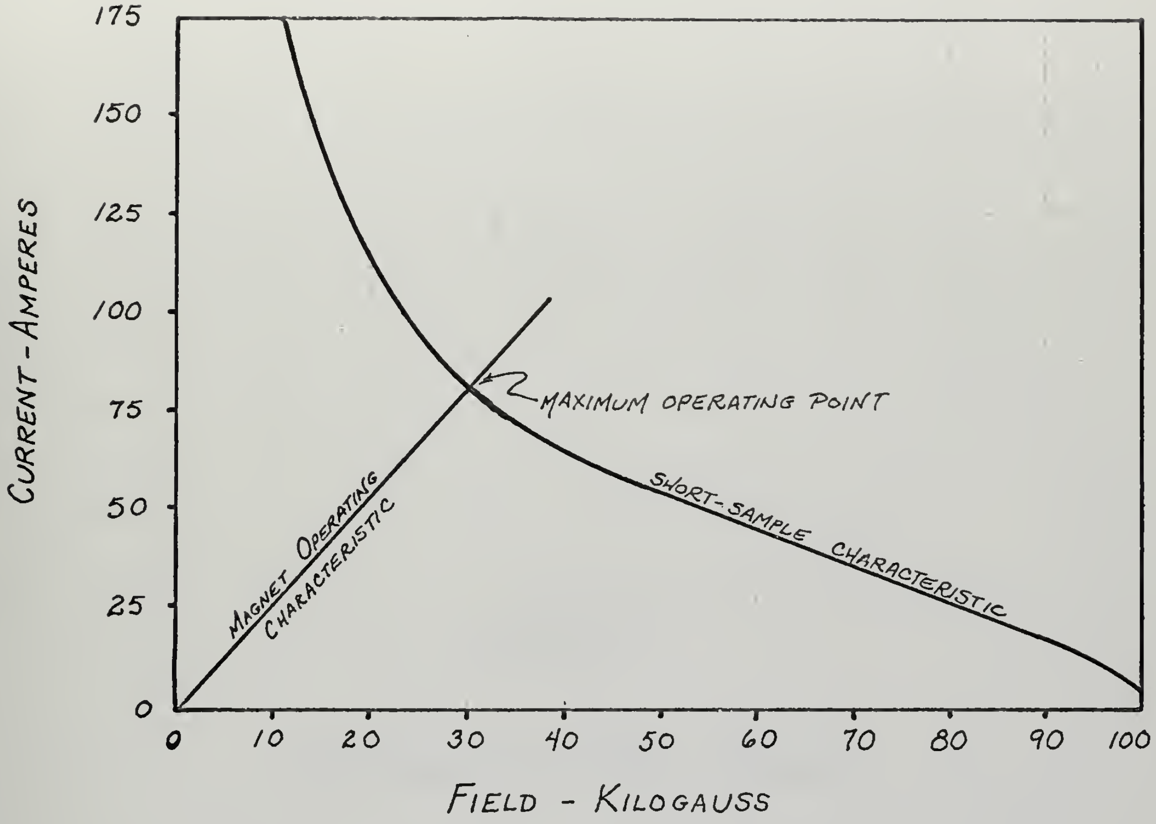

Figure D-1. Supergenic Wire Type SG-100D short sample performance characteristic with magnet operating characteristic superimposed.

APPENDIX E

Optimization of Field Geometry

In approaching the design of a superconducting field in which none of the variables of size are initially fixed, it is evident that higher field intensities will be obtained as the machine size is increased, since there is no longer any limitation imposed by saturation of ferromagnetic material. The quenching field strength of the conductor can also be controlled by varying the geometry of the conductor. Therefore, it is assumed that in practical machine design (4), the objective which must be met by the rotor is that it produce the maximum field, subject to a given outside diameter and fixed volume of conductor. In the generator system, this objective translates to the requirement that the torque produced be a maximum. Figure E-1 illustrates the field geometry to be optimized, namely the values of δ and R_1 are sought.

The torque can be expressed by the integral

$$T = \int_V (\bar{J} \times \bar{B} \times \bar{\rho})\rho \, d\rho \, d\phi \, dl ,$$

where $\bar{B}$ is the field produced in the armature and $\bar{J}$ is the current density of the field. From (1) the fundamental component of the radial flux density inside the armature, per phase, is given by

$$B_\rho = \frac{3\mu_0 J_a}{2\pi} (R_o - R_i) \cos (\phi - \psi).$$

Then $\bar{J} \times \bar{B} = \dfrac{3\mu_0 J_f J_a}{2\pi} (R_o - R_i) \cos (\phi - \psi)$ in the axial direction.

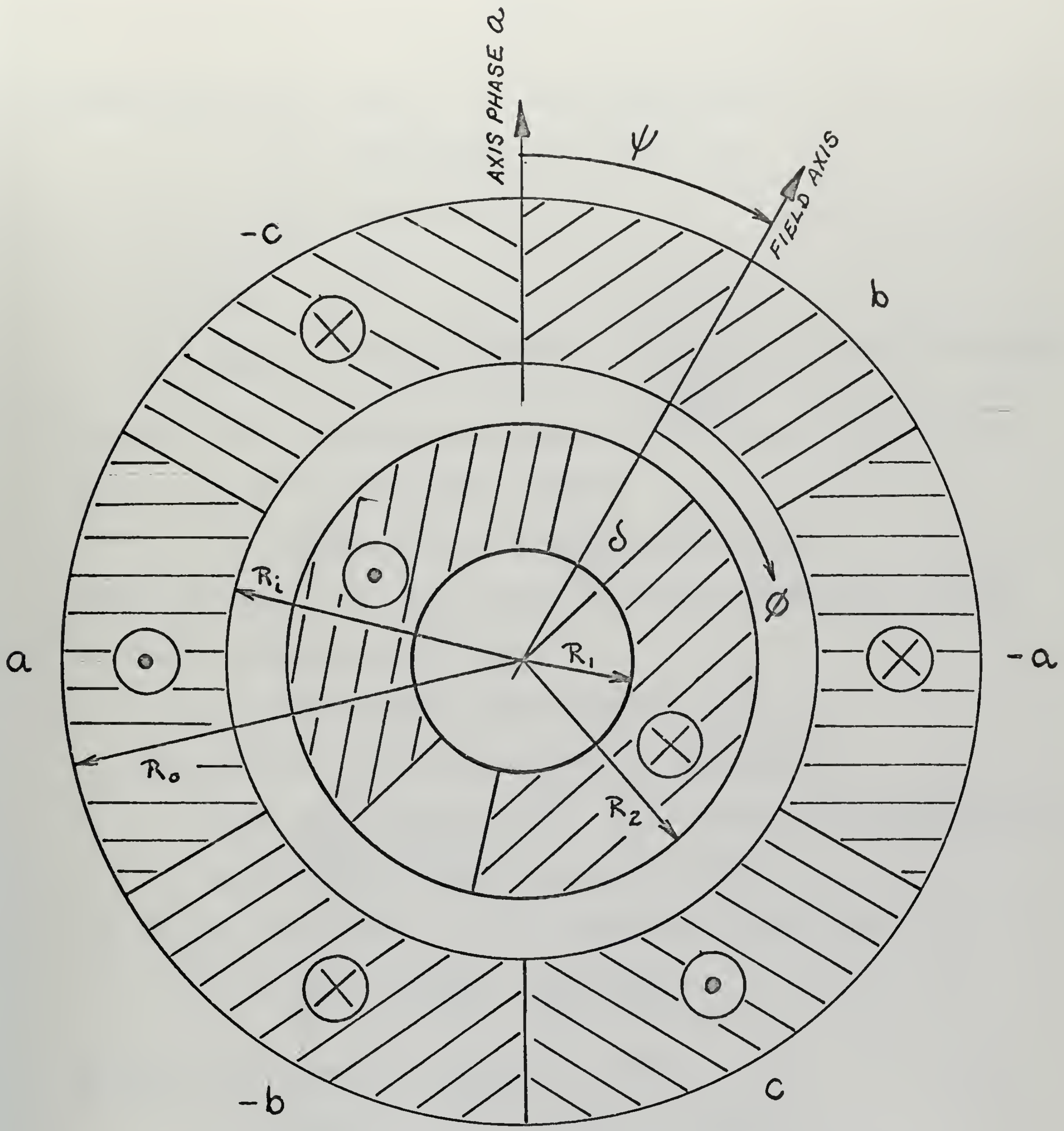

Figure E-1. Nomenclature for Field Geometry Optimization.

Since $\bar{J}_f = + J_f$ for $\delta < \phi < 180 - \delta$

$- J_f$ for $180 + \delta < \phi < 360 - \delta$

0 elsewhere,

the integral becomes

$$T = \int_{R_1}^{R_2}\int_{\delta}^{180-\delta} \frac{3\mu J_f J_a}{2\pi}(R_o - R_i)\rho^2 \sin\phi \, d\rho \, d\phi - \int_{R_1}^{R_2}\int_{180+\delta}^{360-\delta} \frac{3\mu J_f J_a}{2\pi}(R_o - R_i)\rho^2 \sin\phi \, d\rho \, d\phi$$

assuming that the maximum torque is delivered for $\psi = 90^\circ$.

Evaluation of the integral yields

$$T = \frac{2\mu}{\pi} J_f J_a \, (R_o - R_i)(R_2^3 - R_1^3) \cos\delta$$

This expression for the torque is to be maximized, subject to the following constraints:

1. a fixed outside rotor radius, $R_2 = r_o$
2. a fixed volume of conductor, N_f, where

   $N_f = \frac{\pi\lambda}{2a_c}\left(\frac{90 - \delta}{90}\right)(R_2^2 - R_1^2)$, with a packing factor λ and conductor cross-sectional area a_c.

The second constraint can be rewritten in the form

$$\delta = \frac{\pi}{2} - \frac{N_f a_c}{\lambda} \cdot \frac{1}{(R_2^2 - R_1^2)}$$

If $k_1 = I_f/J_f$ and $k_2 = \frac{2\mu}{\pi} J_a k_1$, then

$$T\,(R_1, R_2, \delta) = k_2 \, I_f \, (R_2^3 - R_1^3) \cos\delta \, .$$

The constraints may be written in functional notation as

1. $F\,(R_1, R_2, \delta) = \frac{\pi}{2} - k_3 \frac{1}{(R_2^3 - R_1^3)} - \delta = 0$,

where $k_3 = \frac{N_f a_c}{\lambda}$, and

2. $G\,(R_1, R_2, \delta) = R_2 - r_o = 0$

At an extreme point of the function T,

$$T_{R_1} dR_1 + T_{R_2} dR_2 + T_\delta d\delta = 0 ,$$

$$F_{R_1} dR_1 + F_{R_2} dR_2 + F_\delta d\delta = 0 , \text{ and}$$

$$G_{R_1} dR_1 + G_{R_2} dR_2 + G_\delta d\delta = 0 .$$

The subscripts denote partial derivatives with respect to the variable indicated. If the required operations are performed on the functions T, F, and G, and the resulting values substituted into the partial derivative equations,'a set of homogeneous equations is obtained which may be solved simultaneously. The resulting equation expresses the requirement for maximum torque:

$$-2k_3(R_2^3 - R_1^3)\sin\delta + 3R_1(R_2^2 - R_1^2)\cos\delta = 0.$$

When this equation is combined with the constraints $R_2 = r_o$ and $\delta = \frac{\pi}{2} - k_3 \frac{1}{(R_2^2 - R_1^2)}$, the requirement is expressed in terms of the single variable R_1:

$$-2k_3(r_c^3 - R_1^3)\cos\left(\frac{k_3}{r_o^2 - R_1^2}\right) + 3R_1(R_2^2 - R_1^2)\sin\left(\frac{k_3}{r_o^2 - R_1^2}\right) = 0 .$$

Evaluation of this expression for the outside rotor radius value of 2.5" and $N_f = 5500$ turns leads to an optimum torque when $\delta = 10^\circ$ and $R_1 = 1.875''$.

BIBLIOGRAPHY

1. Woodson, H.H.; Stekly, Z.J.J.; et al. "Research and Design of Superconductive and Cryogenic Electronic Power Generator; Final Technical Report". Avco-Everett Research Laboratory, January 1965.

2. Scurlock, R.G. Low Temperature Behavior of Solids. Dover Publications, New York, 1966.

3. Wang, Chi-Teh. Applied Elasticity. McGraw-Hill, New York, 1953.

4. Greeneisen, D.P. "A Design Program for Superconducting Machines". Electrical Engineering M.S. Thesis, M.I.T., May 1968.